

## Collective membrane motions in the mesoscopic range and their modulation by the binding of a monomolecular protein layer of streptavidin studied by dynamic light scattering

Rainer Hirn, Roland Benz, and Thomas M. Bayerl\*

*Universität Würzburg, Physikalisches Institut EP-5, 97074 Würzburg, Germany*

(Received 25 November 1998)

Using a dedicated dynamic light scattering setup, we have studied the angstrom-scale amplitude undulations of freely suspended planar lipid bilayers, so-called black lipid membranes (BLM's), over a previously not accessible spread of frequencies (relaxation times ranging from  $10^{-2}$  to  $10^{-6}$  s) and wave vectors ( $250 \text{ cm}^{-1} < q < 35\,000 \text{ cm}^{-1}$ ). This allowed a critical test of a simple hydrodynamic theory of collective membrane modes, and the results obtained for a synthetic lecithin BLM are found to be in excellent agreement with the theoretical predictions. In particular, the transition of the transverse shear mode of a BLM between an oscillatory or propagating regime and an overdamped regime by passing through a bifurcation point was clearly observed. It is shown that the collective motions in the time- and wave-vector regime covered are dominated by the membrane tension, while membrane curvature does not contribute. The binding of the protein streptavidin to the BLM via membrane anchored specific binders (receptors) causes a drastic change in frequency and amplitude of the collective motions, resulting in a drastic increase of the membrane tension by a factor of 3. This effect is probably caused by a steric hindrance of the transverse shear motions of the lipid by the tightly bound proteins. [S1063-651X(99)13705-X]

PACS number(s): 87.15.He, 87.15.Kg, 87.15.Ya

### INTRODUCTION

Thermally excited undulations or, more general, collective motions are considered as crucial contributors to the short-range interaction potential between cell membranes or between membranes and solid surfaces. They are well characterized in the low-frequency regime for cells (e.g., erythrocytes) and for large unilamellar vesicles (LUV's) as membrane models. The methods used at low frequencies are based on microscopic interferometry coupled with video data acquisition where the restricted bandwidth of the latter limits the access to motions with frequencies beyond 100 Hz.

However, there is a lack of data on collective motions in the mesoscopic and high-frequency range, mainly due to the scarcity of suitable experimental methods. The only experimental proof of the existence of collective membrane motions in the high-frequency regime (upper gigahertz range) so far was obtained by coherent quasielastic neutron scattering (QENS) [1]. In the mesoscopic range, solid state NMR methods have been used to measure collective motions, but, as in the case of QENS, sensitivity problems and the need for using highly oriented samples restrict their application to stacks of model membranes. NMR has the additional disadvantage that it can only detect time correlations not spatial ones, which constrains data analysis. The use of proteins for studying their effect on collective membrane motions is prohibited for NMR and QENS for preparatory reasons: It is extremely difficult to prepare oriented membrane stacks with proteins homogeneously distributed in a functional state over the sample and only a very few successful attempts have

been published. If anionic lipids, which exist in rather high proportions in natural membranes, are to be included, the problem of obtaining oriented bilayers becomes even more complex. On the other hand, there exists a large body of theoretical work on collective membrane motions and the resulting membrane microelastic properties that require for validation experimental methods covering selectively a wide range of frequencies, particularly the mesoscopic range (KHz–GHz).

Dynamic light scattering (DLS) has been suggested as a method to overcome many of the above limitations for studying collective motions of planar bilayers, so-called black lipid membranes (BLM's) [2], and of free soap films in air [3]. However, despite a good theoretical background [4], the technical restrictions on the experimental layout did not allow the DLS technique to show its full potential for such studies, mainly due to a lack of sensitivity at higher frequencies. We have recently suggested a dedicated DLS experiment that overcomes the limitations of the past by a different setup design and improved sample preparation techniques. The technique can cover a wave-vector range from  $250$  to  $35\,000 \text{ cm}^{-1}$  ( $1.8 < \lambda < 250 \mu\text{m}$ ) and a time scale of four orders of magnitude (from  $6 \times 10^{-3}$  to  $6 \times 10^{-7}$  s). This broad wave-vector and time regime is sufficient for testing theories of membrane undulations and enables new experiments on the effects of the coupling between proteins, peptides, or polymers and the membrane on collective membrane dynamics. Another advantage of the method is that BLM's are systems that are under considerable lateral tension, in contrast to LUV's, which are tension free. Thus curvature effects that are dominating features in the collective motions and micromechanics of LUV's are negligible in BLM's.

In this work we have addressed the problem of how the collective motions of a BLM are altered after the tight coupling of a water soluble protein to its surface. This is a situ-

\*Author to whom correspondence should be addressed. FAX: 49-931-888-5851.

Electronic address: bayerl@physik.uni-wuerzburg.de

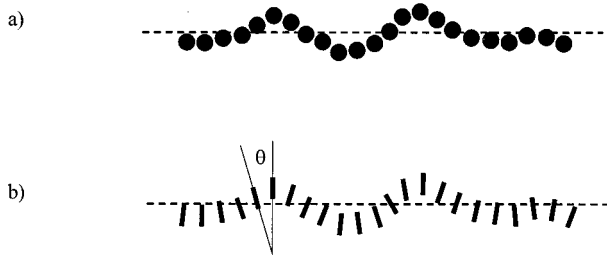


FIG. 1. Schematic depiction of (a) the transverse shear mode of a membrane consisting of isotropic molecules as treated by Kramer and of (b) the transverse shear mode coupled with the splay mode of a membrane consisting of anisotropic molecules, as considered in the extension of Kramer's theory by Fan.

ation that is quite common in biological systems for the specific binding between ligands and membrane anchored receptors. We have chosen the protein streptavidin, which is well established in binding biotin groups linked to phospholipids at exceptionally high binding affinity and can form a monomolecular protein layer on top of a biotin functionalized bilayer surface. Using DLS, we have studied collective motions of a biotin-functionalized BLM of dielaidoyl-sn-glycero-phosphocholine (DEPC) prior to and after the streptavidin binding.

### THEORY

The undulation behavior of freely suspended planar membranes in solution was theoretically treated about 30 years ago by Kramer [4]. He postulated that in a certain wave-vector regime the angstrom-scale amplitudes of selected membrane undulation modes of thin elastic membranes are detectable by DLS.

Kramer treated all interactions as linear functions and completely ignored the anisotropic structure and dynamics of the lipid molecules, owing to their partial ordering in the bilayer. In summary, he made the following approximations:

- (i) All hydrodynamic equations (i.e., Navier-Stokes) are linear.
- (ii) The fluid surrounding the membrane symmetrically is incompressible.
- (iii) The membrane elastic properties can be described by compression and shear moduli and a membrane tension like a two-dimensional solid with isotropic molecules.
- (iv) At the membrane-fluid interface the velocities of the two media are the same.
- (v) The fluid velocity becomes zero at large distances from the membrane.
- (vi) The wavelength of the collective modes is large compared to the membrane thickness and small compared to its diameter.

For the special case of a membrane consisting of isotropic molecules symmetrically immersed in a homogeneous liquid it was concluded that the transverse shear mode is the only collective motion accessible by DLS on a physically meaningful time scale. All other modes are either completely insensitive to DLS or exist at higher frequencies only (gigahertz range and higher), which are hardly resolvable by state-of-the-art autocorrelators. As is depicted in Fig. 1(a), the transverse shear mode describes the out of plane motions of

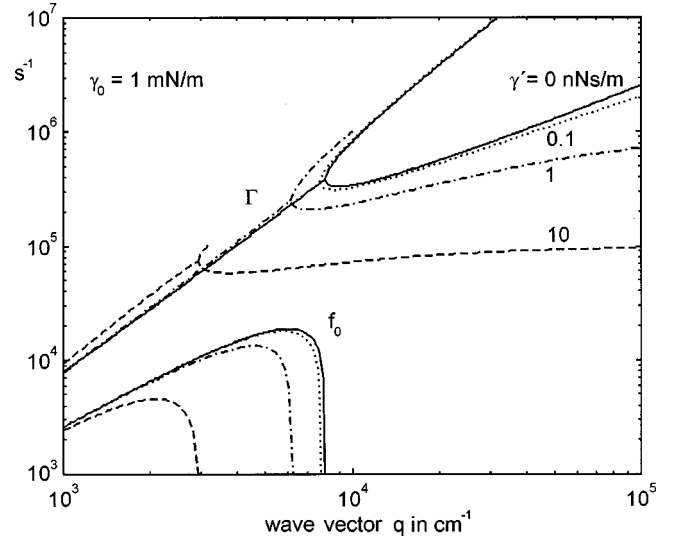


FIG. 2. Plot of Eq. (1) in the wave-vector range accessible by DLS for a membrane tension  $\gamma_0 = 1$  mN/m, a fluid density  $\rho = 1$  mg/ml, and fluid viscosity of  $\eta = 1$  mPas for different surface viscosities  $\gamma' = 0$  nNs/m (—),  $0.1$  nNs/m (···),  $1$  nNs/m (·-·), and  $10$  mNs/m (---).

isotropic molecules. For the case of a BLM, this would lead to an effective fluctuation of the membrane area. This gives rise to a dynamic membrane tension that is characteristic of the shearing process. This renders the collective BLM motion tension dominated, and the dispersion relation of this transverse shear mode is given by

$$2m\rho\omega^2 + \gamma q^3(q - m) = 0, \quad (1)$$

where  $m = (q^2 - i\rho\omega/\eta)^{0.5}$ ,  $q = 2\pi/\lambda$  is the scattering vector,  $\omega = \omega_0 - i\Gamma$  is the complex frequency consisting of the eigenfrequency  $\omega_0$  and the damping constant  $\Gamma$ ,  $\rho$  and  $\eta$  are the density and viscosity of the fluid, and  $\gamma = \gamma_0 - i\omega\gamma'$  is a complex tension with the real part being the membrane tension and  $\gamma'$  the surface viscosity.

Figure 2 shows a plot of  $\omega_0$  and  $\Gamma$  versus  $q$  according to Eq. (1) using parameters typical for BLM's. A detailed discussion of this dispersion equation is given in [2]. For BLM's with tensions in the range  $0.1 < \gamma_0 < 4$  mN/m the left-hand side of Fig. 2 describes an oscillating regime, while the right-hand one is characteristic of an overdamped regime. The crossover between the two regimes occurs fairly abruptly and is typically located around  $q = 5000 \text{ cm}^{-1}$ . The damping constant  $\Gamma_0$  in the oscillating regime splits above the transition (bifurcation) point in two branches labeled  $\Gamma_1$  for the slower mode and  $\Gamma_2$  for the faster mode. For higher  $q$  values the slower mode  $\Gamma_1$  moves asymptotically toward the limiting value  $\xi = \gamma_0/\gamma'$ . When the faster mode  $\Gamma_2$  assumes this value it merges into the bulk mode that has the dispersion relation

$$i\omega - \eta q^2/\rho = 0 \quad (2)$$

and vanishes for  $\Gamma_2$  values above  $\xi$ . Because this bulk mode might couple to the fast undulation mode  $\Gamma_2$  it is likely that this thermally driven fast undulation mode dissipates its en-

ergy by this coupling. However, as the bulk mode is insensitive to DLS, a detection of  $\Gamma_2$  is unlikely.

So far, no DLS experiment has been able to measure sufficiently high  $q$  values to cover this transition region, which would provide a critical testing of the still unverified Kramer theory. Equally important are measurements in the overdamped region, where a clear dependence of  $\Gamma_1$  on  $\gamma'$  is predicted.

By additionally considering the geometrical anisotropy of the lipids, Fan extended Kramer's theory [5]. He suggested an additional splay mode coupled to Kramer's transverse shear mode, with a coupling strength depending on the free energy variation arising from tilting the molecular director of a lipid away from those of the adjacent lipids [Fig. 1(b)]. Thus, in Fan's treatment the membrane tension  $\gamma_0$  is no longer a constant but depends on the curvature energy  $\kappa$  and the undulation wave vector  $q$ , giving rise to an effective tension

$$\gamma_{0 \text{ eff}} = \gamma_0 + \kappa q^2. \quad (3)$$

Equation (3) shows that at high  $q$  values  $\kappa$  dominates the undulation behavior. This is identical to the dependence of the effective undulation amplitude  $u_{\text{eff}}$  of a membrane of area  $A$  on the undulation wave vector  $q$ , as described by the famous Helfrich equation [6]

$$\langle u_{\text{eff}}^2(q) \rangle = \frac{kT}{A(\gamma_0 q^2 + \kappa q^4)}, \quad (4)$$

where  $k$  is the Boltzmann constant,  $T$  the absolute temperature,  $\gamma_0$  is the lateral tension, and  $\kappa$  is the curvature energy.

At room temperature and for standard BLM parameters ( $\gamma_0 = 1$  mN/m,  $\kappa = 10^{-19}$  J, diameter  $\mathcal{D}_{\text{BLM}} = 3.5$  mm), an effective undulation amplitude  $u_{\text{eff}} \approx 0.09$  Å can be estimated from Eq. (4) at  $q = 1000$  cm $^{-1}$ . The total amplitude can be estimated by summing up the contributions at all physically reasonable  $q$  values (thickness  $\mathcal{T}_{\text{BLM}} < \lambda/2 < \mathcal{D}_{\text{BLM}}$ ) as  $\approx 10$  Å. Such tiny amplitudes, which are much smaller than the micrometer range amplitudes found in LUV's or in erythrocytes are the result of the significantly higher lateral tension  $\gamma_0$  in BLM's. In the tension dominated regime characterized by the above BLM parameters, the  $\kappa$  contribution is only a millionth of that of the tension and thus negligible. In spite of their tiny amplitude, these tension-dominated undulations are readily detectable by DLS.

Figure 3 shows the deviation from Kramer's dispersion relation due to Eq. (3) in the limit of high  $q$  values. Even at  $q = 300\,000$  cm $^{-1}$  ( $\lambda = 200$  nm) the  $\kappa$  contribution is only one-tenth of that of the tension and thus not measurable experimentally since the maximum  $q$  limit in state-of-the-art DLS is about 35 000 cm $^{-1}$  (see below).

## MATERIALS AND METHODS

### Sample geometry

To perform high quality DLS measurements on BLM's it is of paramount importance that the BLM's be large (several millimeters in diameter) and long-lasting, i.e., stable for days. Our BLM containing a scattering cell is a standard square glass cuvette of 40×10×10 mm (Hellma GmbH &

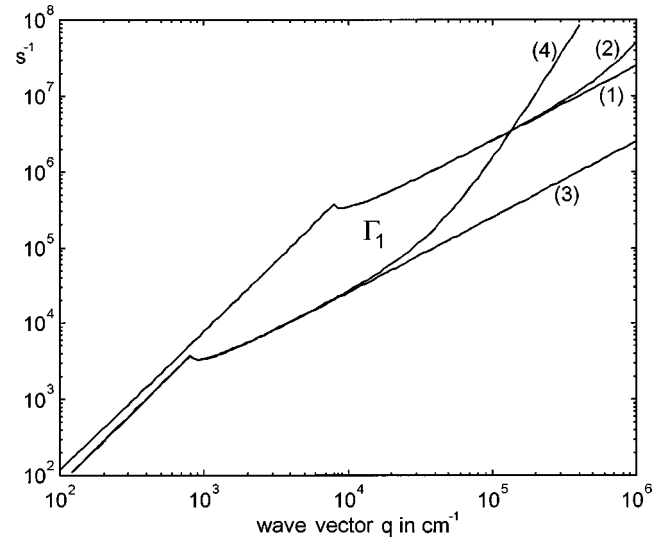


FIG. 3. Comparison of Kramer's theory [Eq. (1)] and Fan's dispersion theory [Eqs. (1) and (2)] for two pairs of  $\gamma_0$  and  $\kappa$  values. For simplicity only the slow damping modes  $\Gamma_1$  are plotted as a function of  $q$ . The two curves with highest slope at high  $q$  values (curves 1 and 2) show the effect of curvature according to Fan. The parameters used in the calculations are  $\gamma_0 = 1$  mN/m and  $\kappa = 0$  J (curve 1),  $\gamma_0 = 1$  mN/m and  $\kappa = 10^{-19}$  J (curve 2),  $\gamma_0 = 0.1$  mN/m and  $\kappa = 0$  J (curve 3), and  $\gamma_0 = 0.1$  mN/m and  $\kappa = 50 \times 10^{-19}$  J (curve 4).

Co., Mühlheim, Germany). A rectangular Teflon wall of 2 mm thickness and having a hole of 4.5 mm in its center, divides the cell diagonally into two compartments. Across this hole a 25  $\mu$ m thick Teflon foil with a 3.5 mm hole (the BLM bearing hole) is attached concentrically using a Teflon frame mount. We found that the use of the thin foil and the 3.5 mm wide bearing hole provides the conditions required for having a widely planar and stable BLM allowing high  $q$  resolution and eliminating any laser reflections from the Teflon. Moreover, the low thickness of the foil prevents positional fluctuations of the BLM as a whole, which would otherwise reduce the  $q$  resolution. The long-time stability of the BLM (a typical membrane lasted for more than two days) was achieved by subjecting the foil to hole drilling techniques that give a hole edge that appears perfectly smooth by light microscopy inspection.

Capillary waves of the water surface were eliminated by a suitable stopper in the upper part of the cell ( $\approx 1$  cm above the BLM bearing Teflon hole) in direct contact with the water. The cuvette was mounted inside a water circulating system for controlling the cell temperature (22 °C for all measurements) via a water bath thermostat (Neslab Instruments Inc., Portsmouth, NH).

### Membrane preparation

BLM's were formed by gliding a Teflon loop carrying the film forming solution [1% (wt./vol.) of lipid dissolved in *n*-decane] over the 3.5 mm Teflon hole. The *n*-decane 99+% (Sigma-Aldrich Chem. GmbH, Steinheim, Germany) was additionally purified using an alumina column until it was completely colorless. The water level in the scattering cell was adjusted to 3 mm above the upper edge of the Teflon wall, thus eliminating hydrostatic pressure differences. Prior to

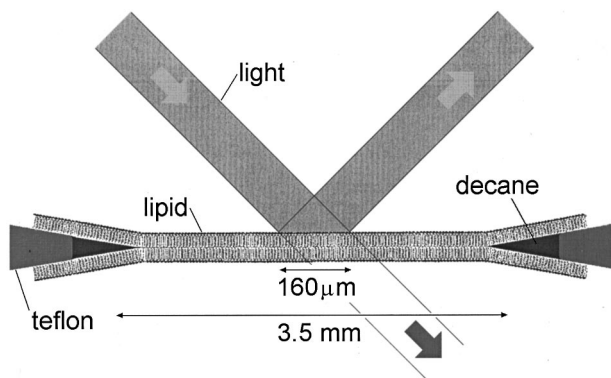


FIG. 4. Schematic depiction of the BLM in the Teflon hole with respect to the illuminated scattering area (not to scale).

this the hole was pretreated by spreading a methanol solution containing 2% (*w/v*) lipid on it followed by solvent evaporation in air. After formation, the BLM's were allowed to equilibrate overnight before measurements commenced. By observing slow positional variations of the reflected laser spot, we established a slow relaxation of the BLM, which came to equilibrium about 8 h after its formation. The phospholipids used were 1,2 dielaidoyl-sn-3-glycerophosphocholine (DEPC) from Avanti Polar Lipids, Inc. (Alabaster, AL) and *N*-(6-(biotinyl)amine)-hexanoyl-dipalmitoyl-phosphatidylethanolamine (B-cap-DPPE) from Molecular Probes, Inc. (Eugene, OR). They were used without further purification. Streptavidin (Sigma-Aldrich Chem. GmbH) was dissolved (1 mg/ml) in the same buffer as used in the BLM cell (20 mM Hepes buffer *pH* 7.2 containing 50 mM KCl) and added in equal amounts to both sides of the BLM using a microsyringe. The buffer solution used in the scattering cell was previously degassed and filtered through a 0.1- $\mu\text{m}$ -diam sterile filter of polycarbonate (Millipore Corp., Bedford, MA) to remove dust particles.

### Experimental setup

The argon ion laser used (Innova 70-4 from Coherent Inc., Santa Clara, CA) was operated on its shortest line (457.9 nm, TEM<sub>00</sub>) at 150 mW and the polarization of the beam was parallel to the membrane. The laser beam was focused on the BLM using a lens of 50 cm focal length to achieve a small angle of divergence (0.11°) and thus high  $q$  resolution. The illuminated spot on the BLM (scattering area) had a diameter of 160  $\mu\text{m}$  (Fig. 4). The photomultiplier (PM) was mounted on a goniometer arm (PM and goniometer both from ALV GmbH, Langen, Germany) at an angle of 45° with respect to the BLM normal and at 30 cm distance from the scattering area. The  $q$  regime of interest was selected by placing a pinhole ( $\varnothing$  700  $\mu\text{m}$ ) near the BLM and a second one ( $\varnothing$  80  $\mu\text{m}$ ) right in front of the PM. For higher  $q$  values ( $q > 3400 \text{ cm}^{-1}$ ) the 80  $\mu\text{m}$  pinhole was replaced by a vertical slit aperture (2000  $\times$  200  $\mu\text{m}$ ) to collect additionally the out of plane scattering intensity. The reasoning for using the slit aperture is as follows. Undulations like the transverse shear mode represent plane waves  $u(r, t)$  with

$$u(r, t) = u_0 e^{-i(qr + \omega t)}, \quad (5)$$

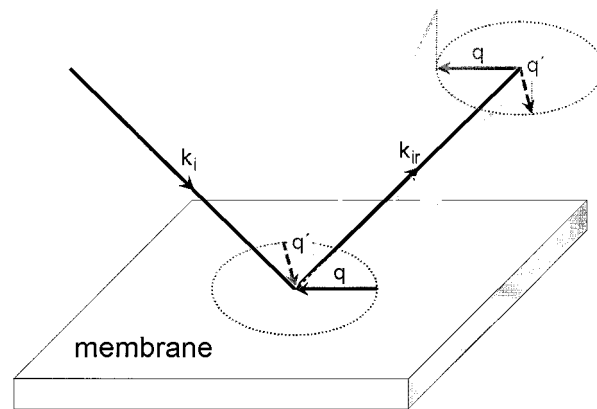


FIG. 5. Schematic depiction of the DLS scattering geometry showing the incident vector  $k_i$  and specular reflected vector  $k_{ir}$  (scattering angle 45°), the in-plane wave vector  $q$ , the in-plane scattered vector  $k_s$ , the out-of-plane wave vector  $q'$ , and the out-of-plane scattered vector  $k'_s$ . Note that the modulus of the scattering vector remains approximately constant, while its component along the membrane plane is changed by the vector  $q$ .

which travel along all directions parallel to the membrane. In the membrane plane, all possible  $q$  vectors belonging to the same undulation mode are confined within a circle (cf. Fig. 5), giving rise to both in-plane and out-of-plane scattering of the incident light vector  $k_i$ . However, owing to the inclination of the detector plane (the plane perpendicular to the specular reflected vector  $k_{ir}$ ) by 45° with respect to the membrane normal, the region of scattered vectors  $k_s$  at the detector site can be approximated to first order by an elliptical slit aperture having an aspect ratio of 2<sup>0.5</sup> in front of the detector, with  $k_{ir}$  pointing through its center. To avoid the use of elliptical slit apertures for each single  $q$  value for obtaining the out-of-plane scattering intensity, the PM is simply rotated around the center of the BLM, i.e., the ellipse is approximated by its tangent for a given  $q$  value. This tangent is formed by the slit aperture. In this case the relative error in selecting the desired  $q$  value has its maximum of 3% at  $q = 3400 \text{ cm}^{-1}$  and is not bigger than what would result from using the 80  $\mu\text{m}$  pinhole at  $q = 900 \text{ cm}^{-1}$ . This approach increases the *S/N* of the detector signal by a factor of 80 without any reduction of signal quality.

The PM signal was preamplified and processed by autocorrelation in 388 channels using an ALV 3000 correlator (ALV GmbH, Langen, Germany). Measurements were done in the heterodyne mode using the diffuse scattering arising from the molecular roughness of the BLM as a local oscillator. The time increments used varied from 0.1 to 10  $\mu\text{s}$ . The whole DLS setup was capsulated for dust protection and mounted on a 200 kg laser table (Melles-Griot, Paris, France), which was shock insulated by four air damping modules.

### Data analysis

In the oscillating regime, the autocorrelation functions  $G(t)$  were fitted to the theoretically expected function [2]

$$G_0(t) = a + b \cos(\omega_0 t + \Phi) e^{-\Gamma_0 t} + ct, \quad (6)$$

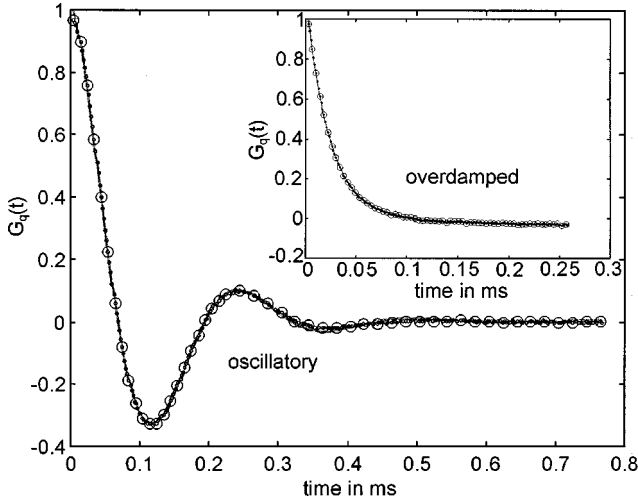


FIG. 6. Examples of typical correlation functions  $G(t)$ , measured in the overdamped and in the oscillatory regime of a DEPC-BLM at 22 °C. The full lines represent fits to the data according to Eqs. (5) and (8).

where  $ct$  is the linear baseline correction and  $\Phi$  is a phase factor. Corrections of  $G_0(t)$  in the limit of small  $q$  to compensate for instrumental effects [2] were not performed, since these deviations from Eq. (5) were found to be completely negligible for  $q > 400 \text{ cm}^{-1}$ .

At the transition point (bifurcation) between the oscillating and overdamped regime and its vicinity ( $q_{\text{bifurcation}} \pm 400 \text{ cm}^{-1}$ ), the data were fitted according to

$$G_t(t) = a + (b + ct)e^{-\Gamma t} + dt. \quad (7)$$

This is the general expression for the asymptotic limit case of classical harmonic oscillators and indicates that in this transition region both overdamped modes  $\Gamma_1$  and  $\Gamma_2$  are detectable. Finally, in the overdamped regime were two damping modes are predicted [Eq. (1)], the data were fitted to

$$G_d(t) = a + be^{-\Gamma_1 t} + ce^{-\Gamma_2 t} + dt, \quad (8)$$

with a linear baseline correction  $dt$ .

However, beyond the point where  $\Gamma_2$  assumes the value  $\gamma_0/\gamma'$ , the fast mode disappears. For  $q$  values beyond this point only the slow mode  $\Gamma_1$  was considered in the fitting procedure. Typical autocorrelation functions measured by DLS at selected  $q$  values corresponding to the damped and to the overdamped regime of the transverse mode of BLM of pure DEPC are shown along with their fits according to Eqs. (6)–(8) in Fig. 6. Measuring autocorrelation functions with a  $S/N$  like that shown in Fig. 6 requires acquisition times between 30 s and 5 h, depending on  $q$  and on membrane tension. The latter is particularly important for high tensions, since the amplitudes and thus the scattering intensity are reduced with increasing tension [Eq. (4)].

Fitting the autocorrelation functions with the appropriate equations (6), (7), or (8) provides the mode frequency  $f_0$  and the damping constant  $\Gamma$ . The relationship between the  $q$  value and the actual scattering angle  $\varphi$  adjusted with the goniometer is given by

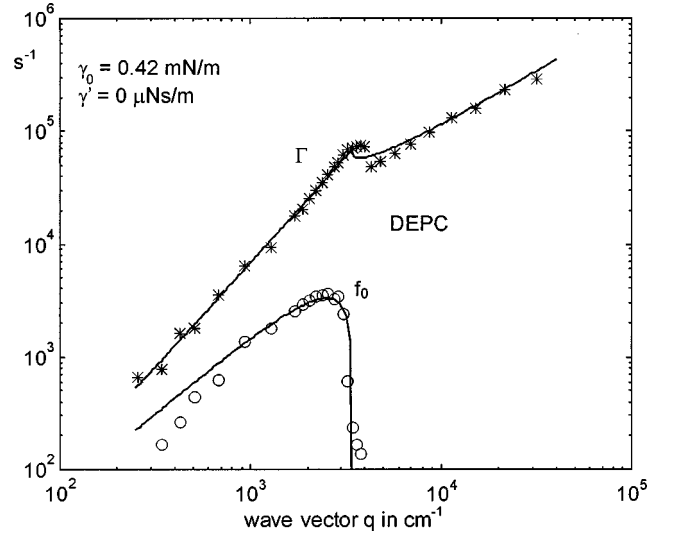


FIG. 7. Mode frequency  $f_0 = \omega_0/2\pi$  (lower curve) and damping constant  $\Gamma$  (upper curve) versus mode wave vector  $q$  of a free planar bilayer (BLM) of DEPC, calculated from the autocorrelation functions measured at the corresponding  $q$  values. The full lines represent the Kramer theory fitted to the data, giving an average lateral tension  $\gamma_0 = 0.42 \text{ mN/m}$  and a negligible surface viscosity  $\gamma'$ .

$$q = n \frac{2\pi}{\lambda} \sqrt{[\sin(\Theta)]^2 + [\sin(\Theta + \vartheta)]^2 - 2 \sin(\Theta) \sin(\Theta + \vartheta)}, \quad (9)$$

where  $n = 1.33$  is the refractive index of water,  $\lambda = 457.9 \text{ nm}$  is the wavelength of the incident laser light,  $\Theta = 45^\circ$  is the static scattering angle,  $\vartheta = \arcsin[\sin(\varphi)/n]$  is the corrected scattering angle (water/air interface), and  $\varphi$  is the variable scattering angle.

## RESULTS

As a first experiment, a pure DEPC membrane was measured at 22 °C. The complete dispersion curve in the range of  $250 \text{ cm}^{-1} < q < 35\,000 \text{ cm}^{-1}$  is shown in Fig. 7. The data are compared with best fits (full lines) according to Eq. (1). From that an average lateral tension  $\gamma_0 = (0.42 \pm 0.03) \text{ mN/m}$  and a negligible shear interfacial viscosity  $\gamma'$  ( $\gamma' < 2 \times 10^{-7} \text{ mN s/m}$ ), acting in the direction normal of the membrane, is obtained. It is obvious that the agreement between experiment and theory is excellent over almost three orders of magnitude in  $q$ . The theoretically predicted transition from the damped to the overdamped case (cf. Fig. 2) is clearly observed experimentally at  $q = 3300 \text{ cm}^{-1}$ . Minor deviations of  $f_0(q)$  from the theory at lowest measurable  $q$  in Fig. 7 can be ascribed to a slight average overall equilibrium deformation of the BLM, giving rise to some diffuse reflection of the incident laser light at lowest  $q$ . Moreover, at  $q < 400 \text{ cm}^{-1}$  there could be a non-negligible contribution arising from the (Gaussian) instrumental function of the setup.

However, there is one striking discrepancy between theory and experiment observed in the overdamped regime (cf. Fig. 7): only one overdamped mode corresponding to the slow mode  $\Gamma_1$  can be fitted to the data, while theory predicts

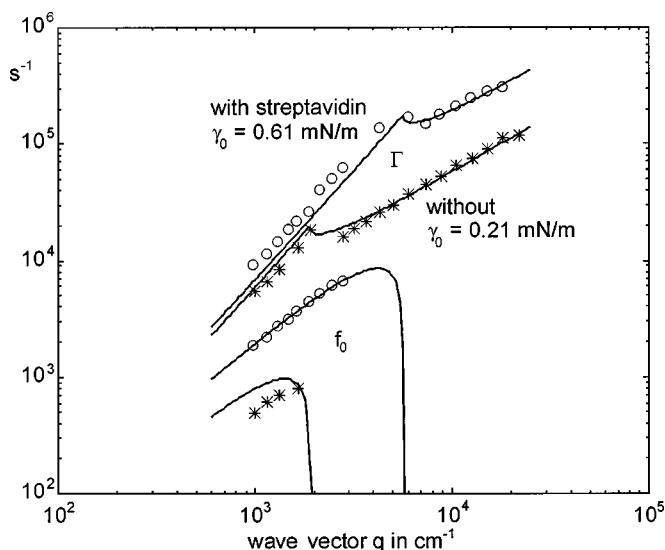


FIG. 8. Mode frequencies  $f_0$  and damping constants  $\Gamma$  versus mode wave vector  $q$  of a DEPC-BLM doped with 5 mol % biotin-cap-DPPE (\*) and of the same membrane after the binding of streptavidin at both sides (O). The full lines are fits according to Eq. (1), giving the average lateral tension of  $\gamma_0 = 0.205$  mN/m prior to and  $\gamma_0 = 0.61$  mN/m after the binding of streptavidin. In both cases the surface viscosity  $\gamma'$  is negligible.

additionally a fast mode  $\Gamma_2$  (Fig. 2). In contrast, around the bifurcation point we were able to extract two modes according to Eq. (7), indicating that there the fast mode  $\Gamma_2$  is indeed detectable but seems to decrease with increasing  $q$  very rapidly.

In a second experiment we have studied the effect of streptavidin binding to the BLM on its collective modes. To achieve tight binding, we prepared a DEPC-BLM containing 5 mol % of Biotin-cap-DPPE. Since streptavidin exhibits four specific binding sites for biotin, we can expect a spontaneous protein binding to the BLM after addition of the streptavidin to the buffer medium surrounding the BLM. Prior to the addition of the streptavidin, we measured the biotin-doped BLM over the full  $q$  range accessible (after the BLM was equilibrated overnight). Then the streptavidin was flushed into the cell under conditions that it could access the BLM from both sides (symmetric binding). Since the streptavidin-biotin binding constant is very high, as is the amount of protein added (0.4 mg/ml), saturation of the BLM should occur rather quickly, controlled by the molecular diffusion of the protein in the bulk. Four hours after the protein injection, we started again a DLS measurement. Figure 8 shows the results for  $f_0$  and  $\Gamma$  vs  $q$  for both cases. We observe a rather drastic effect of the streptavidin binding regarding the  $q$  value at which the crossover from the damped to the overdamped regime occurs. Fits to the data according to Eq. (1) gave an average lateral tension of  $\gamma_0 = 0.205$  mN/m before and  $\gamma_0 = 0.61$  mN/m after binding of the streptavidin, i.e., a factor of 3 increase in lateral tension. As a control, we did this experiment again, with the only difference being that the membrane was not doped with the biotinyl-lipid (pure DEPC-BLM). For this case we observed no changes in  $f_0$  and  $\Gamma$  over the full  $q$  range upon addition of the same amount of streptavidin. This shows that the key-lock mechanism of biotin-streptavidin binding is a prerequi-

site for the measurable binding to the BLM surface.

It is noteworthy that the biotin-doped membrane alone shows a 50% weaker tension ( $\gamma_0 = 0.205$  mN/m) than that measured for the pure DEPC membrane ( $\gamma_0 = 0.42$  mN/m). Furthermore, a slight but systematic deviation of the damping constant  $\Gamma$  from the theory can be observed. The latter might be caused by instrumental effects (slight errors in PM positioning at high  $q$ ) as well as by the baseline corrections involved in the analysis of the autocorrelation functions. In spite of these minor deviations the results give us confidence that the collective modes of a BLM alone and in the presence of a protein can be described with a surprising accuracy by the simple hydrodynamic Kramer theory and that curvature effects do not contribute to the mode relaxation in the  $q$  range covered by our experiments.

## DISCUSSION

The results shown in Figs. 7 and 8 allow a critical assessment of the Kramer theory over a sufficiently wide  $q$  range. For a pure DEPC-BLM, this theory describes its viscoelastic dispersion behavior amazingly well over a wide  $q$  range (250–35 000  $\text{cm}^{-1}$ ). For comparison, a previous attempt to measure collective BLM motions by DLS [2] was restricted to the range 600–1800  $\text{cm}^{-1}$  by technical limitations, and thus did not allow observation of the transition from the oscillatory to the overdamped regime. Moreover, we observe a drastic change of the dispersion behavior for the case in which a protein binds tightly to the BLM via a receptorlike group anchored to the membrane.

In more detail, we can draw the following conclusions. (i) The dispersion behavior of the BLM's studied is clearly dominated by the lateral tension at negligible surface viscosity. (ii) Curvature effects do not contribute to the dispersion behavior in the  $q$  range studied. (iii) In spite of the otherwise excellent agreement between experiment and theory, only the slow one of the two theoretically predicted overdamped modes  $\Gamma_1$  and  $\Gamma_2$  [Eq. (8)] is detectable by DLS. (iv) The binding of streptavidin to the BLM causes a significant reduction of amplitude of the transverse shear mode and an increase of the lateral tension compared to that of a pure DEPC BLM. (v) The protein effect on the BLM collective motions is observed only when specific binders (biotin groups) are anchored to the BLM, which itself lowers the BLM tension by a factor of 2 compared to the pure DEPC BLM.

The failure of our method to detect the predicted fast overdamped mode  $\Gamma_2$  is rather surprising considering the otherwise excellent agreement with theory. While  $\Gamma_1$  describes the slow recovery of the system driven by tension and viscosity,  $\Gamma_2$  is driven essentially by the inertia of the system arising, within the approximations of the theory, from the fluid surrounding the BLM. Although  $\Gamma_1$  is readily detectable in our experiment, relaxation via the  $\Gamma_2$  process is observed only in the vicinity of the bifurcation point. We interpret this discrepancy as due to a non-negligible influence of a surface viscosity  $\gamma'$  (not bigger than  $2 \times 10^{-7}$  mNs/m), which causes a merger of the fast overdamped mode  $\Gamma_2$  with the (DLS insensitive) bulk mode [Eq. (2)]. This merger may give rise to a very fast relaxation of

$\Gamma_2$  at  $q$  values beyond the bifurcation region, rendering it undetectable by DLS in the overdamped regime.

The almost negligible contribution of the surface viscosity  $\gamma'$  to the mode relaxation is probably caused by a more BLM-specific property: the inevitable presence of spurious amounts of apolar solvents (decane in our case) in the bilayer. The thickness of this solvent layer depends directly on the solvent used. For the case of decane, an increase of the BLM thickness by 2 nm compared to a solvent-free lipid bilayer was reported [7]. The presence of this solvent may cause an increase of the internal volume and an effective reduction of the van der Waals interactions between adjacent lipid tails and between the two opposite monolayers, driving the surface viscosity down to very low values. This is confirmed by experiments where the decane was substituted by squalane, which allows the preparation of virtually solvent-free but less stable BLM's. For squalane, we deduced a non-negligible value of  $\gamma'$  by fitting Eq. (1) to the experimental dispersion curve (data not shown). Since long-time stable squalene BLM's required for our protein experiments were not achievable, we used decane as a solvent.

Our experiments are from the methodological approach reminiscent of an earlier work where undulations of free soap films were studied by DLS. In this paper, a linear hydrodynamic theory was presented that was based on assumptions similar to the Kramer theory, but that additionally considered an electrostatic potential in the dispersion relation. A comparison with our data seems inappropriate for the large structural differences between soap films and BLM's and the fact that the former were surrounded by air rather than water. Moreover, the frequency range of the soap film study does not match our study.

The addition of the 5 mol % biotin-cap-DPPE causes a 50% lowering of the BLM tension compared to that of pure DEPC (Fig. 8). This effect can be understood in terms of the increase in area/molecule due to the presence of the bulky biotin groups linked by a short spacer to the DPPE head group. Note that the area per biotin-cap-DPPE is 120–160 Å<sup>2</sup> [8] and thus more than 30% larger than that of a DEPC molecule. Hence, the presence of Biotin- $x$ -DPPE may create additional free volume for the DEPC molecules and lower the van der Waals interaction between adjacent lipid chains, leading to an increased amplitude of the collective modes and a decreased tension.

The effect of the streptavidin binding is quite the opposite. The tension increases well above that of a pure DEPC-BLM by the protein binding to the biotin groups. The exceptionally high affinity between biotin and streptavidin, with a binding constant comparable only to that of covalent bonds [9], ensures that once a bond is formed there are only two alternatives left: either the protein stays attached to the BLM for a long period of time or it detaches by pulling the biotin-cap-DPPE bound to it out of the bilayer. The energy required to achieve the dissociation of a monomeric lipid from the bilayer is very high compared to the thermic energy [10]. Moreover, since we have on average two biotin-cap-DPPE's available in each BLM monolayer per streptavidin (which exhibits two binding sites accessible from the membrane surface), this energy will be even higher. Therefore we can safely assume that after the incubation with streptavidin, the BLM is symmetrically surrounded by two protein monolay-

ers. Neutron and x-ray measurements on biotin-cap-DPPE doped DMPC monolayers have indicated that the streptavidin monolayer formed is dense and homogeneous over micrometer distances with about 40 Å thickness [11].

The increase in tension of the composite streptavidin-BLM system can be understood by considering two mechanisms. First, the binding pockets of streptavidin allow a rather deep penetration of the biotin into it and, consequently, the protein is pulled down very close to the membrane surface. As one streptavidin covers about 50 DEPC molecules of the BLM [11], it is very conceivable that the protein will drastically reduce the amplitude of the transverse shear modes in the covered DEPC bilayer area simply for steric reasons. This effect may become even more pronounced in the presence of two protein layers "sandwiching" the BLM. Second, it was shown previously that the streptavidin binding to B-cap-DPPE causes a significant dehydration of the lipid head groups [8–14]. This dehydration may increase the molecular order of the BLM lipid chains and consequently the van der Waals interaction between adjacent DEPC molecules. This would result in transverse shear undulations of higher frequency and lower amplitude and thus in an increased tension.

Furthermore, it is remarkable that the Kramer theory describes data well, even after the symmetric binding of the two protein layers. This indicates that the basic hydrodynamics is not significantly changed by this binding. This is probably due to the fact that the binding is symmetric with respect to the bilayer center and that the protein layer formed is smooth on a molecular level. In fact, neutron reflection techniques have demonstrated that the roughness of the streptavidin layer is less than 5 Å and thus not significantly higher than that of a lipid monolayer [8].

## CONCLUSIONS

We have shown that the DLS technique can detect collective membrane modes in BLM's over a broad wave-vector and time range and can be used for a critical test of hydrodynamic theories of membrane undulations. The significant changes observed for the case of a tight protein binding to the surface of the BLM further demonstrates the usefulness of the method for obtaining insight into the dynamic consequences of the specific binding between a membrane bound receptor and a protein. Studies that are presently performed in our laboratory using different proteins indicate that the dynamical response of the BLM upon interaction with the corresponding protein depends strongly on the particulars of the molecular interaction. Thus, it will be possible to distinguish certain interaction mechanisms by the DLS method.

## ACKNOWLEDGMENTS

The authors are indebted to Professor Lorenz Kramer (Universität Bayreuth) for many helpful discussions. This work was supported by grants from the Deutsche Forschungsgemeinschaft (DFG) and the Hertie Foundation.

- [1] W. Pfeiffer, S. König, J. F. Legrand, T. Bayerl, and E. Sackmann, *Europhys. Lett.* **23**, 457 (1993).
- [2] J. F. Crilly and J. C. Earnshaw, *Biophys. J.* **41**, 197 (1983).
- [3] A. Vrij, J. G. Joosten, and H. M. Fijnaut, *Adv. Chem. Phys.* **48**, 329 (1981).
- [4] L. Kramer, *J. Chem. Phys.* **55**, 2097 (1971).
- [5] C. Fan, *J. Colloid Interface Sci.* **44**, 369 (1973).
- [6] W. Helfrich and R.-M. Servuss, *Nuovo Cimento D* **3**, 137 (1984).
- [7] J. Dilger and R. Benz, *J. Membr. Biol.* **85**, 181 (1985).
- [8] D. Vaknin, K. Kjaer, H. Ringsdorf, R. Blankenburg, M. Piepenstock, A. Diederich, and M. Lösche, *Langmuir* **9**, 1171 (1993).
- [9] P. C. Weber, D. H. Ohlendorf, J. J. Wendolowaki, and F. R. Salemme, *Science* **243**, 85 (1989).
- [10] C. A. Hehn, W. Knoll, and J. N. Israelachvili, *Proc. Natl. Acad. Sci. USA* **88**, 8169 (1991).
- [11] M. Lösche, M. Piepenstock, A. Diederich, T. Grunewald, K. Kjaer, and D. Vaknin, *Biophys. J.* **65**, 2160 (1993).
- [12] E. Evans and S. Simon, *J. Colloid Interface Sci.* **51**, 266 (1975).
- [13] S. White, *Biophys. J.* **23**, 337 (1978).
- [14] C. Dolainsky, A. Möps, and T. Bayerl, *J. Chem. Phys.* **98**, 1712 (1993).